

Prime Number Selection of Cycles in a Predator-Prey Model

ERIC GOLES,† OLIVER SCHULZ,* AND MARIO MARKUS*

†Center for Mathematical Modelling of Complex Systems, FCFM, University of Chile, Casilla 170-3, Santiago, Chile

*Max-Planck-Institut für molekulare Physiologie, Postfach 500247, D-44202 Dortmund, Germany

Received September 14, 2000; revised January 30, 2001; accepted January 30, 2001

The fact that some species of cicadas appear every 7, 13, or 17 years and that these periods are prime numbers has been regarded as a coincidence. We found a simple evolutionary predator-prey model that yields prime-periodic preys having cycles predominantly around the observed values. An evolutionary game on a spatial array leads to travelling waves reminiscent of those observed in excitable systems. The model marks an encounter of two seemingly unrelated disciplines: biology and number theory. A restriction to the latter, provides an evolutionary generator of arbitrarily large prime numbers. © 2001 John Wiley & Sons, Inc.

1. INTRODUCTION

The appearance of three species of the genus *Magicalca* synchronously every 13 or 17 years and asynchronously every 7 years [1,2] has not been convincingly explained. These cicadas spend most of their lives below the ground, emerging and dying within a few weeks. The present work is based on the hypothesis that the cycle length is a prime number in order to optimally escape predators. For example, a prey with a 12-year cycle will meet—every time it appears—properly synchronized predators appearing every 1, 2, 3, 4, 6 or 12 years, whereas a mutant with a 13-year period has the advantage of being subject to fewer predators. According to R. MacArthur [1], this idea may be the only application of number theory in mathematical biology; a drawback, however, is that there is as yet no evidence for relevant periodic predators of cicadas. Nevertheless, Lloyd and Dybas [3] pointed out that the predator hypothesis can be maintained by assuming para-

sitoids that attack eggs or adults, which may have become extinct. Models of periodical cicadas presented so far [4,5] show that synchronized periodical behavior is possible for periods longer than 10 years. An alternative mechanism to the predator hypothesis is given (without model calculations) by Yoshimura [6,7]; he argues that prime numbers are selected because these cycles are the least likely to co-emerge and hybridize, so that they prevent genetic breakdown by breeding synchrony. This mechanism has been compared [8] with that proposed by Cox and Carlton [9], which also involves advantage of prime cycles due to less frequent hybridization.

The purpose of the present work is twofold: (i) we want to underline that in spite of missing biological data supporting the predator hypothesis, a simple, purely temporal model does lead to locking into prime-periodic prey cycles, whereas a spatiotemporal model leads to a maximum probability of such cycles; (ii) one can use these biological ideas

for a nonbiological, purely number-theoretical goal, namely to construct an evolutionary algorithm yielding prime numbers of any size. In addition, one can consider the present work from the viewpoint of an evolutionary game [10] including spatial dimensions; such a viewpoint sets a link to phenomena reported for spatial versions of the Prisoner's dilemma [11–13], the hawk-dove game [14], and prebiotic evolution [15].

2. SIMULATION OF TEMPORAL PROCESSES

We now set up a model considering first a predator of period X interacting with a prey of period Y . We assign a momentary fitness $f_y(t)$ of the prey in a year t as follows: it is zero if it is not present, it is -1 if both predator and prey are present, and it is $+1$ if the prey is present but the predator is not. Note that we punish prey that appears and meets a predator ($f_y(t) = -1$), compared with the case of nonemergence of the prey ($f_y(t) = 0$); we do this because emergence uses up metabolic resources, because of metamorphosis, mating, and death; these resources are lost if the prey is eaten up by a predator, whereas they are preserved if the prey stays as larvae below the ground. The momentary predator fitness $f_x(t)$ is defined analogously as for the prey, but with opposite signs. The fitness F_x , resp. F_y , is defined by the sum over the $f_x(t)$, resp. $f_y(t)$, $t = 0, \dots, XY$, divided by the number of predator, resp. prey, generations. (Note that this yields an average valid for $t \rightarrow \infty$, because the process is periodic with period XY .) We divided by the number of generations because we found that no such division favors short generation times, instead of properly timed generations (prime cycle lengths). This is important if one considers that each generation uses considerable metabolic energy, as mentioned above, and these expenses should be minimized in the long run. Assuming that prey larvae can survive for a long time below the ground, our model favors seldom emergences, as long as the prey is safe when it appears. A similar reasoning applies to the predator, e.g., fungi attacking eggs of prey; such a predator can survive for a long time as spores, and our model favors seldom appearances, as long as they get nourishment when they appear. Nevertheless, this model does not cause the cycles to become longer and longer, because prey cycles eventually get locked into a prime number, as we will show below, bringing evolution to a stop.

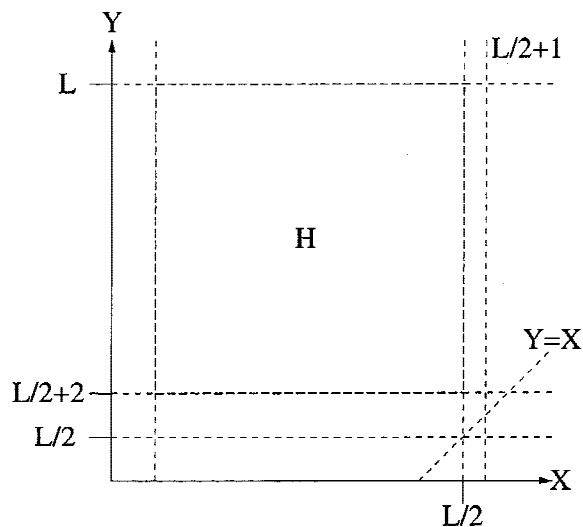
We compare now a prey mutating to a cycle Y' with the resident prey (cycle length Y) at constant X . Analogously, we compare mutant cycles X' with resident cycles X at constant Y . (Note that we do not restrict cycle length changes to ± 1 .) A mutant prey (resp. predator) substitutes the resident if and only if $F_{y'} > F_y$, resp. $F_{x'} > F_x$. Thus, in the case of fitness equality, the resident and not the mutant is selected. Here and in the rest of this work, we assume that all interacting populations are synchronized, thus being all present at $t = 0$.

Now we proceed to analyze the model described in the previous paragraph. Let $lcm(X, Y)$: least common multiple, $gcd(X, Y)$: greatest common divisor of X and Y . In XY years, the predator appears Y times, both predator and prey appear $XY/lcm(X, Y)$ times; thus, predator without prey appears $Y - XY/lcm(X, Y)$ times. Considering that $gcd(X, Y) \cdot lcm(X, Y) = XY$, we thus obtain the predator fitness $F_x(X, Y) = 2gcd(X, Y)/Y - 1$. Analogously, one obtains the prey fitness $F_y(X, Y) = 1 - 2gcd(X, Y)/X$.

We will now show the following: if we allow random mutations—which can be of any size, as long as they lead to mutants within the ranges $2 \leq X \leq L/2$, $L/2 + 2 \leq Y \leq L$ —then a sequence of such mutations will finally lock the prey into a stable prime period Y . We call H the domain defined by these allowed ranges of X and Y . The definition of H on the $X - Y$ plane is given in Figure 1.

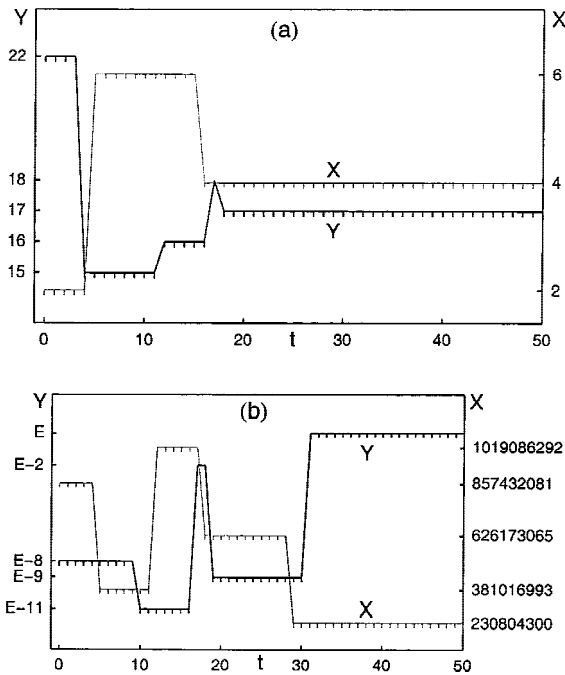
To be more precise, we will show that if Y is not a prime, then there exists a sequence of mutations that will change Y , and if Y is prime, then no mutation will change it. Let us first assume that $Y = Y_N$ is not a prime; $F_x(X, Y_N)$ has the maximum value $2gcd(X_M, Y_N)/Y_N - 1$ at the predator period $X_M = gd(Y_N)$ (gd : greatest divisor). Note that $1 < X_M < L/2 + 1 \rightarrow (X_M, Y_N) \in H$. A sequence of random mutations keeping $Y = Y_N$ constant will eventually lead to X_M . However, (X_M, Y_N) is abandoned if mutations lead to $(X_M, Y_N \pm 1)$. In fact, $gcd(X_M, Y_N) = X_M$, implying that $F_y(X_M, Y_N) = -1$; $gcd(X_M, Y_N \pm 1)$ cannot be equal to X_M (the reason is: $(Y_N \pm 1)/X_M = Y_N/X_M \pm 1/X_M$, the first term being an integer, but the second not, so that X_M is not a divisor of $Y_N \pm 1$) and $gcd(X_M, Y_N$

FIGURE 1



Definition of the domain H within which mutations of X (predator cycle length; abscissa) and Y (prey cycle length; ordinate) are allowed.

FIGURE 2



Evolution to the prey period $Y = 17$ (a) and to $Y = E = 2147483647$ (b); prime number discovered by Euler through mutation-selection sequences (abscissa: number of time steps t ; left ordinate: prey period Y ; right ordinate: predator period X).

± 1) can certainly not be larger than X_M ; thus $\gcd(X_M, Y_N \pm 1) < X_M$; this implies that $F_y(X_M, Y_N \pm 1) > -1 = F_y(X_M, Y_N)$. So far, we have shown that there exists a sequence of mutations such that a prey with a nonprime cycle $Y = Y_N$ is extinguished. Assume now that $Y = Y_p$ is a prime; any $X = X_R$ such that $(X_R, Y_p) \in H$ satisfies the condition $1 \leq X_R \leq Y_p - 1$ and is thus relatively prime to Y_p ; therefore $\gcd(X_R, Y_p) = 1$, so that starting from $(X_R, Y_p) \in H$, there exist no predator mutants that are fitter than a resident. On the other hand, $\gcd(X_R, Y) \geq 1$, where Y is a prey mutant, as compared to $\gcd(X_R, Y_p) = 1$, so that $F_y(X_R, Y) \leq F_y(X_R, Y_p)$, i.e., no prey mutant is fitter than a resident. In conclusion, if H contains a prime prey cycle length, any initial random choice of $(X, Y) \in H$ will lead and lock to a prime Y after a sufficiently large number of mutations. This locking into primes is illustrated in Figure 2. Figure 2a is intended to illustrate a biological process, so we chose a low value of L ($L = 22$) and obtained locking at $Y = 17$. In contrast, Figure 2b is intended to demonstrate a case of number-theoretical relevance, so we chose $L = 2.2 \times 10^9$ and obtained locking of Y into the Euler prime E .

At this point we would like to comment on our restriction to the domain H . We imposed this restriction because the points (jY_p, Y_p) , where Y_p is prime and $j = 1, 2, 3, \dots$, are

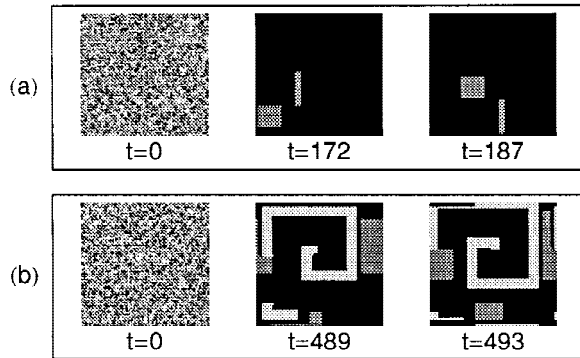
unstable with respect to prey mutations. This can be shown easily: $\gcd(jY_p, Y_p) = Y_p$, whereas $\gcd(jY_p, Y_p - k)$ with $k = 1, 2, 3, \dots$ cannot be larger than $Y_p - k$; thus $F_y(jY_p, Y_p) < F_y(jY_p, Y_p - k)$. This means that convergence to a prey with period Y_p is not possible if mutations to the points (jY_p, Y_p) are permitted. In order to discard these points, one could restrict the system to points above the diagonal $X = Y$. This, however, is not plausible if we want the model to be applicable to biological systems; in fact, this would mean that the limits for prey cycle lengths depend on predator cycle lengths, and vice versa. Such dependences are avoided by restricting mutations to the rectangle H . In addition, H fulfills the requirement that it contains $X_M = \gcd(Y_N)$ (see above).

Note that, as a purely number-theoretical game, i.e., without biological considerations, one may loosen the restriction to the domain H and allow any mutations that lead to (X, Y) pairs above the main diagonal $X = Y$. The restriction then would read $2 \leq X < Y$.

3. SPATIO-TEMPORAL SIMULATIONS

We will now modify the model so that prime numbers are selected by competition between neighboring residents in a spatially extended system, instead of competition between mutants and residents. In this spatio-temporal model there are no random mutations; instead we start the process with cycles X and Y that are randomly distributed in space. Figure 3 shows results obtained with a cellular automaton (CA) evolving from such a random configurations in a two-dimensional habitat with cyclic boundary conditions. The CA is updated after a time Δt , which is equal to the *lcm* of all X and Y at time t in the CA. At time $t + \Delta t$, the predator and the prey of each cell are replaced by the fittest among the neighbors. The neighbourhood is defined by the cell itself, and the eight cells around it. We call C_i ($i = 1, \dots, 9$) the 9 neighbors of C . The momentary fitness $F_x(t)$ of a predator in the time step t is computed here as follows: $f_x(t) = 0$ if the predator does not appear in C_i in that time step; if the predator appears in C_i and the number ν of cells in the 3×3 neighbourhood of C_i occupied by prey is not zero ($1 \leq \nu \leq 9$), then $f_x(t) = \nu$; $f_x(t) = -p$ if the predator appears in C_i and $\nu = 0$. p is a natural number describing a "punishment" for a predator that appears but finds no prey at all. The momentary fitness $f_y(t)$ of the prey is computed analogously, but with opposite signs. The fitness F_x , resp. F_y , of a predator, resp. prey, in C_i are given by the sum of the $f_x(t)$, resp. $f_y(t)$, over all t , t ranging from 1 to the product of all 9 cycle lengths interacting in the neighborhood of C_i ; this sum is then divided by the number of generations of the predator, resp. the prey. In order to update X and Y for a cell C , we perform the evaluation just described in all 9 neighboring cells C_i . We then replace X , resp. Y , in C by the value of X , resp. Y , of the cell C_i that yielded the largest fitness F_x , resp. F_y .

FIGURE 3



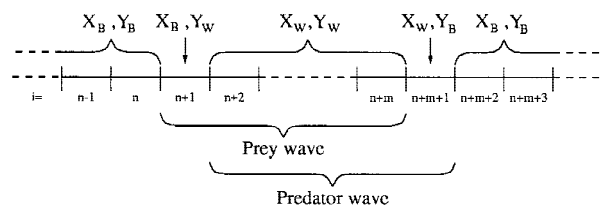
Spatiotemporal dynamics of the cellular automaton starting from a random distribution and evolving to gliders (a) and to a periodic attractor consisting of a rotating spiral surrounded by pulsating smaller domains (b). At $t = 0$, one predator (with cycle X) and one prey (with cycle Y) are placed in each cell by random choice within $\sqrt{E} < X < E - 2$, $E - 8 < Y < E + 8$, where E is the Euler-prime (see Figure 2b). Number of cells: 64×64 . Only Y is shown here. Different grey shadings correspond to different Y , black corresponding to $Y = E$.

The CA just described yields a large diversity of coexisting attractors, depending solely on the choice of the initial, randomly distributed cycle lengths. As in the “Prisoner’s Dilemma” CA [11], the fate of each cell depends here on 25 neighbors; in fact, the fitness of each cell is evaluated by the encounters among the inhabitants of this cell and of its 8 neighbors, but after each time step the inhabitants of a cell are replaced by those having the largest fitness, considering the fitness of that cell and that of each of its 8 neighbors. This contrasts with Conway’s “Game of Life” [16], where only 9 cells specify a cell’s fate. After a sufficient number of CA updatings, we obtain homogeneity, traveling waves (including “gliders” as those shown in Figure 3a), spiral waves (Figure 3b) and periodical, complicatedly pulsating areas, such as those surrounding the spiral in Figure 3b. Because all solutions display periodicity (traveling waves do so because of the cyclic boundary conditions), the existence of an attractor is numerically well defined. We found a predominant appearance of prime-periodic preys, either in the waves or in the background. In the examples given in Figure 3 it is the Euler prime E that appears (black) in the background of the figure. Our particular choice of initial, randomly distributed Y —which is given in the caption—aimed toward the locking into the large prime E . A larger interval of initial Y values causes locking into other primes. As in the work of Hassel et al. [17], the emergent patchiness allows, as in nature, the persistence of otherwise unstable populations, coexisting in space.

The traveling waves can be better understood by considering a CA with only one spatial dimension. We call the

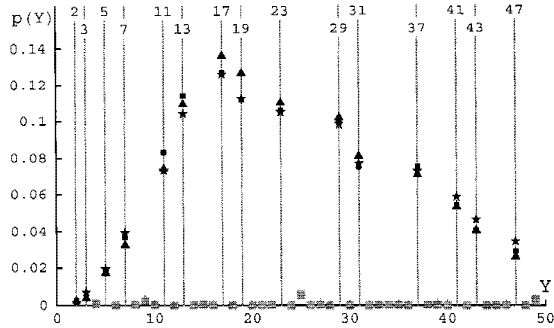
cycles in the background X_B, Y_B and those in the wave X_W, Y_W . This is graphically explained in Figure 4. A one-dimensional wave is composed of five zones defined on the cells denoted by $i = 1, 2, \dots, n, \dots, n + m, \dots$, where $m > 2$ is the width of the wave: (i) X_B, Y_B at $i = 1, 2, \dots, n$; (ii) X_B, Y_W at $i = n + 1$; (iii) X_W, Y_W at $i = n + 2, \dots, n + m$; (iv) X_W, Y_B at $i = n + m + 1$; (v) X_B, Y_B at $i = n + m + 2, \dots$. Note that the predator wave ($i = n + 2, \dots, n + m + 1$) is displaced one cell to the right relative to the prey wave ($i = n + 1, \dots, n + m$); this determines the moving direction to the right, as we will explain now. Considering that predator-prey interactions occur here only with the two immediate neighbors of each cell, the predator at $i = n + m + 1$ (resp. at $i = n + 1$) can feed on two types of prey and thus has a larger fitness than the predator at $i = n + m + 2$ (resp. at $i = n + 2$), which can only feed on one type of prey; therefore, the predator wave will move one cell to the right in the next time step. The prey at $i = n + m + 1$ (resp. the prey at $i = n + 1$) can be eaten by two types of predators and thus has a lower fitness than the prey at $i = n + m$ (resp. at $i = n$), which can only be eaten by one type of predator; therefore, also the prey wave will move one cell to the right. In two dimensions the mechanism is more complicated (especially for gliders moving diagonally, as in Figure 3a), but they can be understood by the same type of reasoning steps. It is remarkable that one-dimensional waves and spiral waves here show a behavior similar to waves in excitable media, such as chemical reactions, heart muscle, and epidemics (see e.g., Refs. 18–22 and references therein). This functions as follows: the spatial domain, which is in the excited state, becomes refractory; the domain in the refractory state becomes excitable; the domain in the excitable state becomes excited; and then the cycle starts again. Also in the spirals found here, there are three spatial domains characterized by cycle pairs (X_1, Y_1) , (X_2, Y_2) , and (X_3, Y_3) that undergo a similar cycle: by virtue of our fitness criterion, the first replaces the second, the second replaces the third, and the third replaces the first; this sequential replacements cause the revolving of the wave. (Note that grey levels only display Y in Figure 3). Spiral

FIGURE 4



Spatial distribution of cycle lengths for a one-dimensional traveling wave (X_W, Y_W) and for the background (X_B, Y_B). i , cell index. The wave moves to the right.

FIGURE 5



Probabilities $P(Y)$ that prey periods Y are selected after the cellular automaton has converged to an attractor. At $t = 0$, cycle lengths are randomly chosen within $2 \leq X, Y \leq 50$ and randomly distributed among 10×10 cells. 10,000 different initial spatial configurations are evaluated. Symbols corresponding to prime, resp. nonprime, Y values are shown in black, resp., gray. Squares: $p = 5$, i.e., predators emerging but getting no prey lose the average of what they would gain (between 1 and 9) if they found prey in the neighborhood; analogously: prey emerging but meeting no predators gain the average of what they would lose (between 1 and 9) if predators emerge in the neighborhood. Triangles: $p = 0$, i.e., predators emerging but finding no prey are undisturbed, whereas prey emerging but meeting no predators are not rewarded. Stars: modified model, so that $f_x(t) = +1$ if the predator emerges and finds prey, independently of the number v of prey-populated neighboring cells (satiation effect) and $f_x(t) = -1$ if emerging prey meets predators, no matter how many.

waves are also obtained in host-parasitoid dynamics [17] and in prebiotic evolutionary automata [15].

We investigate now the capability of our CA to produce prime numbers. For this, we determine the probabilities $P(Y)$ that different prime Y values appear in the attractors of the CA. Figure 5 shows results of such analyses. One clearly sees there a much more frequent appearance of prime prey cycles (dark symbols), especially with periods around 17, compared with nonprime prey cycles (grey symbols, all being very close to the abscissa). This result is robust to drastic variations of the model, these variations being displayed by the symbol shapes in Figure 5 (squares, triangles, and stars) and by Figure 6. Note that in the spatiotemporal model leading to Figures 5 and 6, we only restrict populations by upper bounds ($2 \leq X, Y \leq U$; $U = 50$ in the case of Figures 5, 6b, and 6c; $U = 100$ in the case of Figure 6a).

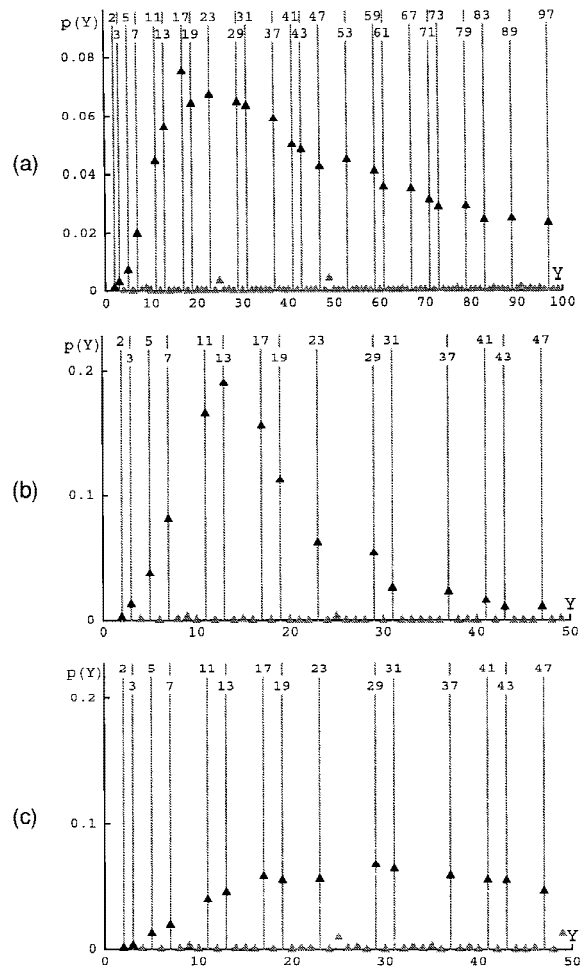
We investigated the influence of the upper bound U and of the grid size of the CA for $p = 5$ (ranges: $25 \leq U \leq 200$; grid size between 10×10 and 30×30). We found that none of these parameters change the peak-like shape of $P(Y)$ vs. Y . Moreover, the value of Y for which $P(Y)$ is maximum is a prime number, independently of U and the grid size. In Figure 6 we show examples for the influence of these parameters. Note that the maximum is attained at $Y = 17$ in Figure 6a and at $Y = 13$ in Figure 6b. In contrast to these

results, a 5×5 grid has more than one maximum: local maximum again at $Y = 17$ and a global maximum at $Y = 29$, the latter being a prime cycle length that has not been observed for cicadas; note that for this small grid, nonprimes ($Y = 25$ and $Y = 49$) are selected with higher probabilities than for larger grids. Moreover, we found that such non-prime selection becomes increasingly more pronounced as the grid is further reduced. Thus, a 10×10 grid (as in Figures 5 and 6a) or a 20×20 grid (as in Figure 6b) are larger than the smallest square grid for which our results are valid.

4. DISCUSSION

Qualitatively, the peak shapes illustrated in Figure 5 and 6 are explained as follows. Prey with sufficiently small Y are exposed to predators having periods $jY \leq U, j = 1, 2, 3, \dots$

FIGURE 6



Results from the same model as that corresponding to the squares in Figure 5 (10×10 cells, $U = 50$), but with different grid sizes and upper bounds of cycles. (a) 10×10 cells, $U = 100$; (b) 20×20 cells, $U = 50$; (c) 5×5 cells, $U = 50$.

the number of such predators decreases on increasing Y , roughly explaining the left branch of the $P(Y)$ peak. Note in this context that we showed above that the pairs (jY_p, Y_p) , where Y_p is prime, are unstable. By virtue of this, the prey with $Y = 17$ is subject to the predators with $X = 17$ and with $X = 34$; however, the number of (initially equally probable) favorable predators is sufficiently large to allow for a maximum of $P(Y)$ at $Y = 17$ in Figures 5 and 6a. In order to explain qualitatively the right branch of the peak, let us compare a large prime Y (say $Y = 47$ in Figure 6b) with a medium prime (say $Y = 13$). As the CA proceeds in time, the prey with $Y = 47$ will favor the survival of one predator in its spatial neighborhood, namely that having $X = 47$, because only this predator can feed well on this prey; however, this predator will meet the prey in each prey generation and will thus strongly decimate the prey; if this prey appears, then $F_y \approx -\nu$. The prey with the smaller $Y = 13$ will favor three types of predators in its spatial neighborhood, namely those with $X = 13, 26$, and 39 . If we make the simplification that these three are equally distributed, i.e., each has an average number $\nu/3$ in the prey's neighborhood and if we consider that $X = 26$ only hits the prey every second prey generation and $X = 39$ only every third prey generation, then the fitness of the prey (which is evaluated per prey generation) is $F_y \approx -\nu(1 + 1/2 + 1/3)/3 = -\nu(11/18)$. Thus, the prey with $Y = 13$ is fitter than that with $Y = 47$, exemplifying the decrease of $P(Y)$ at large Y (right side of the peak). We leave it as an open task to formalize these explanations of the peaks, which are based so far only on estimates and on empirical observations in the course of our CA simulations.

Our results, both from the purely temporal and from the spatiotemporal model, suggest that there are generic properties of this type of dynamics that favor prime numbers. Although there are traditional methods for prime number detection (see e.g., Ref. 23) that are faster than the methods presented here, it is remarkable that the generation of prime numbers can be performed using a biological model.

ACKNOWLEDGEMENTS

We thank the Deutsche Forschungsgemeinschaft and FONDAP (Chile) for financial support. Also, we thank Malte Schmick and David Bressoud for fruitful interactions.

REFERENCES

1. R.M. May. Periodical cicadas. *Nature* 277, 1979, pp. 347–349.
2. J.D. Murray. *Mathematical biology*, Springer, Berlin, 1989.
3. M. Lloyd and H.S. Dybas. The periodical cicada problem. II. *Evolution* 20, 1966, pp. 466–505.
4. F.C. Hoppensteadt and J.B. Keller. Synchronization of periodical cicada emergences. *Science* 194, 1976, pp. 335–337.
5. M.G. Bulmer. Periodical insects. *Am Nat* 111, 1977, pp. 1099–1117.
6. J. Yoshimura. The evolutionary origins of periodical cicadas during ice ages. *Am Nat* 149, 1997, pp. 112–124.
7. A. Barnett. Odd timing keeps cicadas in the prime. *New Sci* 153, March 1997, p. 18.
8. R.T. Cox and C.E. Carlton. A commentary on prime numbers and live cycles of periodical cicadas. *Am Nat* 152, 1998, pp. 162–164.
9. R.T. Cox and C.E. Carlton. Paleoclimatic influences in the evolution of periodical cicadas. *Am Midland Nat* 120, 1988, pp. 183–193.
10. J. Maynard Smith. *Evolution and the theory of games*, Cambridge Univ. Press, 1982.
11. M.A. Nowak and R.M. May. Evolutionary games and spatial chaos. *Nature* 359, 1992, pp. 826–829.
12. M.A. Nowak and K. Sigmund. A strategy of win-stay, lose-shift that out-performs tit-for-tat in the Prisoner's dilemma game. *Nature* 364, 1993, pp. 56–58.
13. A.V.M. Herz. Collective phenomena in spatially extended evolutionary games. *J Theor Biol* 169, 1994, pp. 65–87.
14. M.A. Nowak and R.M. May. The spatial dilemmas of evolution. *Int J Bifurcation Chaos* 3, 1993, pp. 35–78.
15. M.C. Boerlijst and P. Hogeweg. Spiral wave structure in prebiotic evolution: hypercycles stable against parasites. *Physica D* 48, 1991, pp. 17–28.
16. E. Berlekamp, J. Conway, and R. Guy. *Winning ways*, Vol. 2, Academic Press, New York, 1982.
17. M.P. Hassell, H.N. Comins, and R.M. May. Spatial structure and chaos in insect population dynamics. *Nature* 353, 1991, pp. 255–258.
18. V.S. Zykov. *Simulations of wave phenomena in excitable media*, Manchester Univ. Press, 1988.
19. A.V. Holden, M. Markus, and H.G. Othmer, Eds. *Nonlinear wave processes in excitable media*, Plenum, New York, 1991.
20. M. Markus, and B. Hess. Isotropic cellular automaton for modelling excitable media. *Nature* 347, 1990, pp. 56–58.
21. M. Markus, Zs. Nagy-Ungvarai, and B. Hess. Phototaxis of spiral waves. *Science* 257, 1992, pp. 225–227.
22. M. Markus, G. Kloss, and I. Kusch. Disordered waves in a homogeneous, motionless excitable medium. *Nature* 371, 1994, pp. 402–404.
23. P. Ribenboim. *The new book of prime number records*, Springer, New York, 1991.